The Extraction of Time-Invariant Muscle Synergies in the Nociceptive Withdrawal Reflex in the Lower Limb

Barak El-Omar, Ardalan A. Wais, Navinder S. Dhillon and Alari Varmann

Abstract— **Muscle synergies have been investigated in voluntary movements but not in involuntary movements. The present study had two aims: (1) to investigate the muscle synergies in the nociceptive withdrawal reflex (NWR). (2) to investigate how the NWR in the lower limb is affected by electrical stimulation with varying intensity and stimulation sites.**

Surface electromyography (EMG) signals were acquired from 11 healthy subjects. Electrical stimulation was applied on four sites on the plantar side of the foot in order to elicit the NWR. The stimulation was delivered in random order at intensities of 0.7x, 1.1x and 1.7x the pain threshold (PTh) at each stimulation site. Reflexes from the tibialis anterior (TA), gastrocnemius medialis (GA), peroneus longus (PL), rectus femoris (RF) and biceps femoris (BF) were recorded. The time-invariant muscle synergies were extracted using the non-negative matrix factorization (NMF).

The extracted muscle synergies showed the existence of two muscle synergies. The main characteristic of a muscle synergy S1 had a co-activation of TA and PL. Similarly for muscle synergy S2 a co-activation of GA, RF and BF was present. The contribution of each muscle increased with increasing intensity and decreased by changing the sites from 1 to 4. The contribution of each muscle to the synergy was site dependent. This was seen with the different muscle contribution at each site.

The contribution of each muscle synergy were site dependent. There was an increasing activity of PL at site 3 in S1. TA at site 3 and site 4 in S1 was noticeably lower than at site 1 and site 2. It was not possible to quantify the specific movements generated by each muscle synergy in the NWR as the EMG data was normalised.

The investigation indicated that increasing the stimulation intensity would increase the muscle activity in the muscle synergies for each muscle. Furthermore, the change of stimulation site from 1 to 4 altered the muscle activity pattern from a co-activation of TA and PL to GA, RF and BF.

I. INTRODUCTION

The nociceptive withdrawal reflex (NWR) is a spinal reflex that functions to move the limb away from a noxious stimulus [1]. Elicitation of the NWR relies on the stimulation area being within the reflex receptive field (RRF) [2]. Each muscle has its own RRF and multiple muscles can have have overlapping RRF meaning that the NWR response is a net result of the activated muscles overlapping in the RRF [2]. Different stimulation sites on the same limb can thereby result in the contraction of different muscles in order to withdraw the limb. A muscle contraction is the result of activating a neural command signal which originates in different levels of the brain and spinal cord [3]. A Muscle synergy is characterized by a group of muscles recruited by the same neural command signal working toward a common goal. Muscle synergies make it possible to construct a low-dimensional representation of the motor output [4][5].

There are multiple approaches to study the muscle synergies [6]: (1) a single synergy can activate several muscles and a single muscle can engage in multiple muscle synergies and (2) each muscle in a group of muscles contributes to only a single synergy [7]. Muscle synergies can be time-invariant or time-varying. Time-invariant muscle synergies are characterized by having all muscles within that synergy activated at a giving time i.e. no temporal delay is between the muscles. Time-varying muscle synergies contain delays of the muscle activation between muscles within the same muscle synergy [6].

Muscle synergies have been investigated in voluntary movement in animals and humans with regard to specific motor tasks [8][9]. Involuntary movements have been studied with regard to automatic postural responses in humans and withdrawal reflexes in frogs [10] but the NWR response in the lower limb in humans has not been investigated. A method to elicit the NWR response in the lower limb is by electrical stimulation of the foot sole [11]. In this study the surface electromyography (EMG) data of NWR of tibialis anterior (TA), gastrocnemius medialis (GA), peroneous longus (PL), rectus femoris (RF) and biceps femoris (BF) was recorded. A particular method to extract the muscle synergies is by non-negative matrix factorization (NMF). NMF based on the Lee-Seung algorithm [12] which utilises the multiplicative update rule for time-invariant muscle synergy extraction was applied. The result is the synergy matrix $\mathbf{W}$ that expresses the weightings of the individual muscles within each synergy and the synergy activation coefficient matrix $\mathbf{C}$ that expresses the recruitment of each muscle synergy over time [13]. After having obtained the $\mathbf{W}$ and $\mathbf{C}$ matrices, the EMG data is reconstructible in order to represent the accounted variability of each synergy in the muscle activity pattern.

This study addresses a new approach where the contribution of muscle synergies in the NWR is investigated and how the NWR in the lower limbs is affected by electrical stimulation with varying intensity and stimulation sites.

II. METHODS & MATERIALS

A. Subjects

11 healthy volunteers consisting of five males and six females (age 21-24 years) participated in this study. Informed consent was obtained from all the subjects prior to participation. The Declaration of Helsinki was respected. All subjects were asked to refrain from caffeine and alcohol 2 hours prior to the experiment. Strenuous exercise was not allowed 24 hours prior to the experiment.

B. Electrical stimulation

Four stimulation electrodes (700, AMBU A/S) were positioned non-uniformly on the plantar side of the foot (Fig. 1a). An anode (PALS; Axelgaard, Fallbrook, CA, U.S.A) was placed on the dorsum of the foot (Fig. 1b).

Each electrical stimulus was comprised of a constant current pulse train which consisted of five individual 1 ms pulses that were delivered at 200 Hz by an electrical stimulator (NoxiTest IES 230; Aalborg, Denmark). The interstimulus interval (ISI) was set between 5-8 s. Nine stimulations at each site for each intensity resulted in 108 trials per subject. The stimulations were given randomly in three rounds of 36 trials with a 1-2 min. break between each round.

C. EMG recordings

The muscle activity in TA, GA, PL, RF and BF was recorded using EMG. Cross-talk was reduced in the recording of TA, GA, PL and RF by using a double-differential pre-amplifier. A single-differential pre-amplifier was used to record BF. Therefore three recording electrodes (720, AMBU A/S) were positioned in parallel over TA, GA, PL and RF and two recording electrodes were positioned in parallel over BF with an inter-electrode distance of 20 mm and a common reference electrode of the same type was placed on the lateral malleolus (Fig. 1b and Fig. 1c) The EMG signals were amplified up to 10,000 times and filtered using a 2nd order bandpass filter (passband ranged from 5-500 Hz). The signal was sampled at 2 kHz and stored 200 ms pre-stimulus and 1000 ms post-stimulus. For each muscle in the EMG signal the mean was subtracted to remove the DC offset.

D. Experimental procedure

Initially the subject was positioned in a supine position with knee flexed at 35°. The EMG and stimulation electrodes were mounted on the right leg. The experimental session was divided into three parts: (1) The nociceptive withdrawal reflex threshold (NWR-Th) determination, (2) Pain threshold (PTh) determination, and (3) Reflex recording.

1) NWR-Th determination: The NWR-Th was determined at each site using the up-down staircase method [14]; for each site the subject was stimulated with a starting intensity of 1 mA and then increased with a step of 2 mA until a NWR was detected. A NWR was detected if the z score was higher than 12, which was used for all five muscles. The intensity decreased with a step of 1 mA until a NWR was not detectable. Thereafter a set of three ascending and descending estimations of the NWR-Th was obtained by increasing and decreasing with a stepsize of 0.5 mA. The mean of the last two ascending and descending estimations was calculated which resulted in the final NWR-Th for the subject.

2) Pain threshold determination: The PTh was determined at each site using the NWR-Th as the starting intensity. The PTh was first determined at site 1 by stimulating at the NWR-Th intensity found at this site and an increment of 2 mA with an ISI between 3-5 s. The PTh threshold for the site was determined by subjective assessment from the

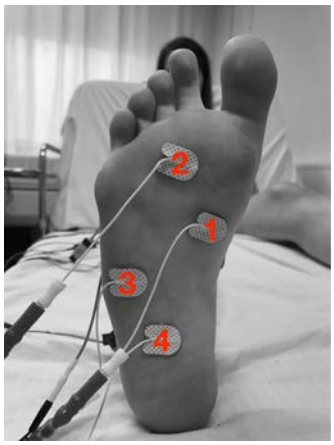

(a)

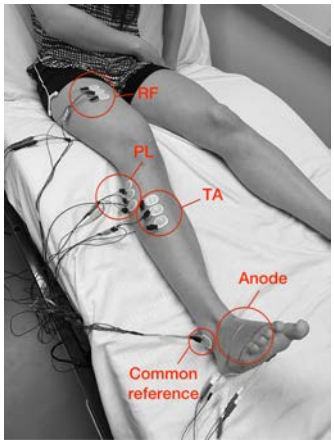

(b)

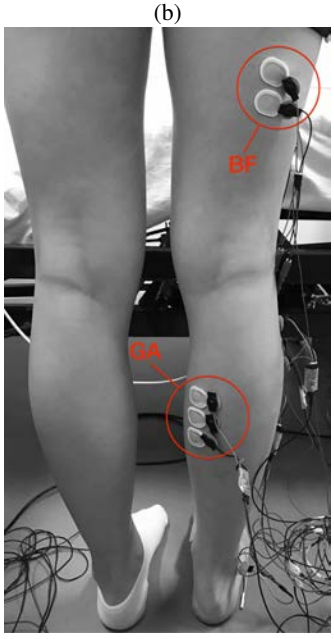

(c)

Fig. 1: (a) Positions of the stimulating electrodes on the four stimulation sites. (b) Subject seated with EMG electodes positioned on TA, PL and RF. The anode is positioned on the dorsum of the foot. (c) Subject with EMG electrodes positioned on the BF and GA.

subject. The subject was asked to tell when the stimulation felt like stepping on a stone, which defined the PTh. The PTh's for the remaining sites were found in a random order. Gradual adaptation at these sites was avoided by intermittently stimulating site 1 at its associated PTh.

3) Reflex recording: Three stimulus intensities (I1, I2, I3) were calculated by multiplying fixed factors by the PTh's determined at each site. The multiplication factors were chosen as 0.7x, 1.1x and 1.7x the PTh. The sequence of stimulation site and intensity for each trial was randomized while the actual reflex recordings were conducted.

E. Data analysis

In order to investigate the contribution of muscle synergies in the NWR under different electrical stimulation intensities and sites, three methods were applied sequentially: (1) Normalization, (2) Linear envelope and (3) Extraction of muscle synergies. All three methods were applied in the reflex window (80-150 ms post-stimulus interval) of the recorded EMG data [15]. The analysis of the recorded signals was conducted using MATLAB (MatLab R2016b, The MathWorks, Inc., USA).

1) Normalization: The data was normalised for each subject by calculating the mean root mean square (RMS) for each muscle across all the 108 trials. The 108 trials for each EMG muscle signal was then divided by the mean RMS. The normalisation made the EMG data comparable across different subjects.

2) Linear envelope: The envelope of the muscle activation was obtained by rectifying and low-pass filtering (4th order Butterworth, cutoff frequency 20 Hz) the normalised EMG data in this sequence. The filtering causes a phase shift in the EMG data, which was removed by performing zero-phase filtering with the built-in `filtfilt` function in MATLAB [9].

3) Extraction of muscle synergies: To extract the muscle synergies, the non-negative matrix factorization (NMF) method was used. The NMF algorithm was implemented with the use of the multiplicative update rule proposed by Lee and Seung [2001] [5].

NMF reduces the dimensions of a matrix by factorizing the matrix of the recorded EMG data $\mathbf{M}$. $\mathbf{M}$ is factorized into two matrices with only non-negative elements, the synergy matrix $\mathbf{W}$ and the synergy activation coefficients matrix $\mathbf{C}$, and a residual error $\mathbf{D}$ which can contain both negative and positive elements [16]. The matrix factorization is given by equation (1)

$$\mathbf{M} = \mathbf{WC} + \mathbf{D} \tag{1}$$

$\mathbf{M}$ is a $m \times n$ matrix (m = number of measured muscles and n = number of samples), $\mathbf{W}$ is a $m \times k$ (k = number of muscle synergies) and $\mathbf{C}$ is a $k \times n$ matrix [13]. $\mathbf{D}$ is the residual error between $\mathbf{M}$ and $\mathbf{WC}$, which is minimized by the factors $\mathbf{W}$ and $\mathbf{C}$ [16]. $\mathbf{D}$ is given by (2)

$$\min_{\mathbf{W},\mathbf{H}} \|\mathbf{M} - \mathbf{WC}\|_F, \quad \text{subject to } \mathbf{W} \geq 0, \mathbf{C} \geq 0 \tag{2}$$

where $\|\cdot\|_F$ is the Frobenius norm. An NMF solver (multiplicative update algorithm in MATLAB) was used in order to reconstruct $\mathbf{M}$ from two matrices, $\mathbf{W}$ and $\mathbf{C}$, with the least $\mathbf{D}$. The multiplicative update rule works in iterations of an initial random estimate of $\mathbf{W}$ and $\mathbf{C}$ that converge to a locally optimal matrix factorization [13]. The number of factorization replicates was 30 for each subject in the algorithm in order to prevent local minima [17][13]. To achieve a consistent extraction of the muscle synergies, the residual convergence criterion and step size was 1e-6 [18], [17]. From all the replicates, the solution with the minimal error needed to reconstruct the EMG data (i.e. the lowest cost solution) was saved [13]. The extent of how much the factorized EMG data could reconstruct the input data for the algorithm was determined by the variability accounted for (VAF) [13][5]. The mean total VAF was given by (3)

$$\text{VAF} = 1 - \frac{\|\mathbf{D}\|_F^2}{\|\mathbf{M}\|_F^2} = 1 - \frac{\sum_{i=1}^{m}\sum_{j=1}^{n}(\mathbf{D}_{i,j})^2}{\sum_{i=1}^{m}\sum_{j=1}^{n}(\mathbf{M}_{i,j})^2} \tag{3}$$

The analysis was iterated by varying the number of muscle synergies, k, between 1 and 5. The least value of k at which a VAF above 95 % could be calculated was chosen as the correct number of muscle synergies needed in order to determine $\mathbf{W}$ and $\mathbf{C}$ as representative of the input data $\mathbf{M}$ [5].

III. Results

A subject-by-subject analysis of VAF indicated that all 11 subjects had a VAF above 95 % at one or two muscle synergies, therefore two muscle synergies, S1 and S2, accounted for at least 95% of the variability of the EMG data. This is shown in Fig. 2.

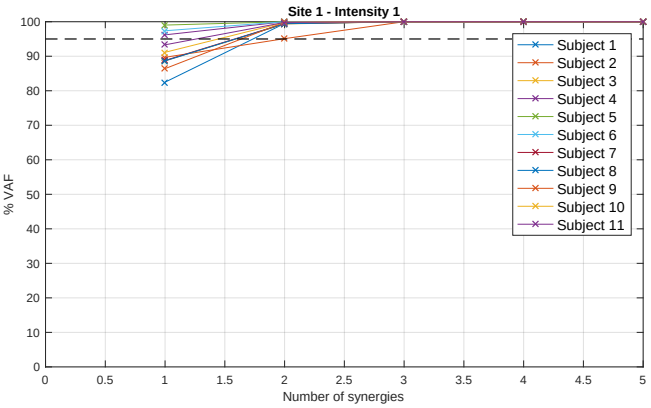

Fig. 2: Illustrating VAF as a function of the number of muscle synergies on individual trial basis for all 11 subjects.

The $\mathbf{W}$ and $\mathbf{C}$ for each site and intensity were extracted for each subject and averaged over subjects. It was assumed that the contribution of each muscle to a particular synergy over all subjects were normally distributed. The $\mathbf{W}$ for S1 is shown in Fig. 3 with the respective $\mathbf{C}$ in Fig. 4 and for S2 the $\mathbf{W}$ in Fig. 5 and $\mathbf{C}$ in Fig. 6.

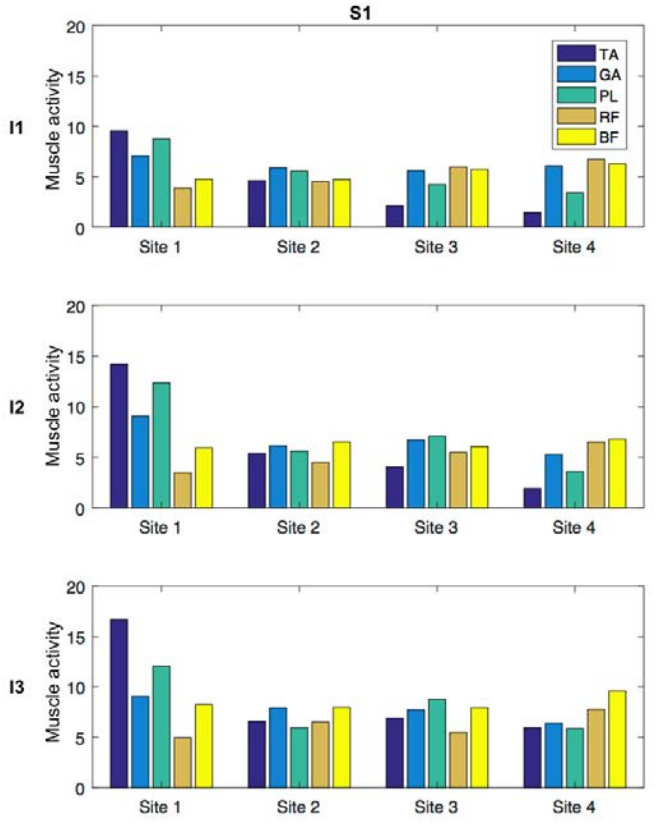

Fig. 3: The average $\mathbf{W}$ in S1 over all subjects.

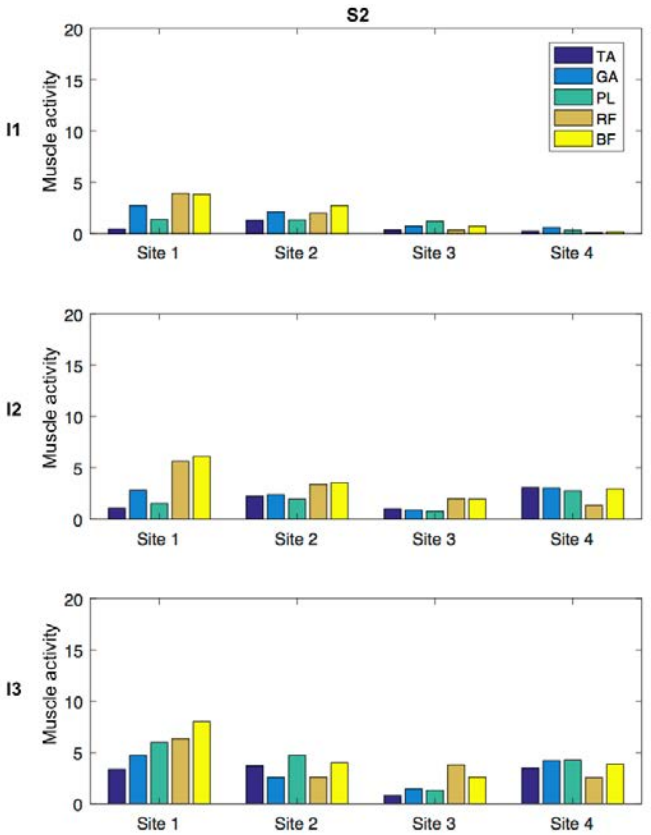

Fig. 5: The average $\mathbf{W}$ in S2 over all subjects.

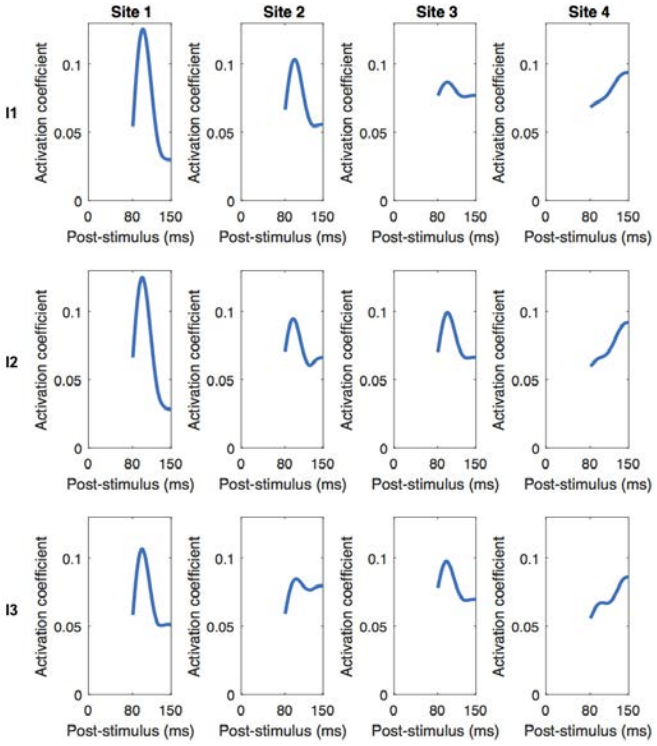

Fig. 4: The average $\mathbf{C}$ in S1 over all subjects.

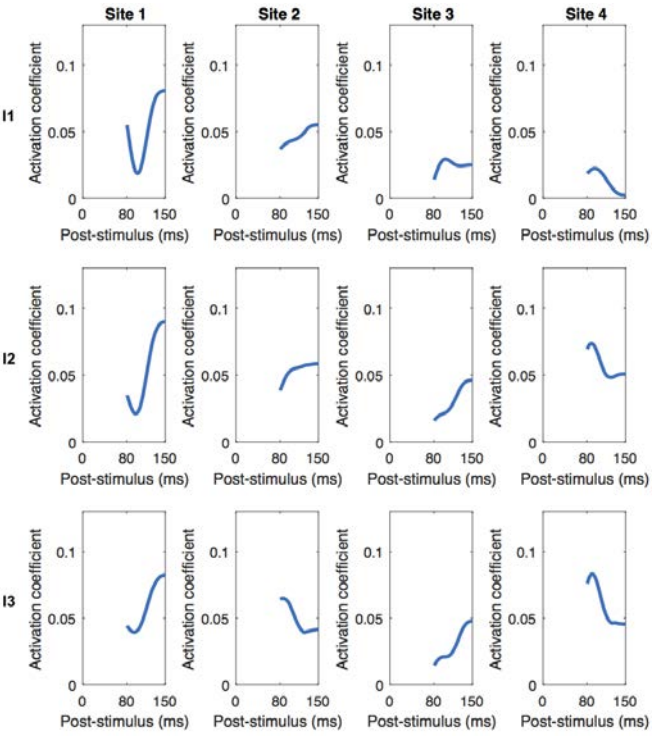

Fig. 6: The average $\mathbf{C}$ in S2 over all subjects.

The results indicated that in most cases, the mean contributions of the muscles to the synergies were increasing with increasing stimulation intensity and decreasing by changing the sites from 1 to 4. In general, the results showed that on the average over subjects, most of the averaged muscle pattern variability was explained by S1.

The results showed that the muscle activation pattern for all intensities at site 1 had a co-activation of TA and PL in S1. As the sites changed from 1 to 4 the muscle activation pattern changed from a co-activation of TA and PL to a more prominent co-activation of GA, RF and BF at all sites at I1 and I2 for S1. Co-activation is defined by the most active muscles in a synergy. In S1 the muscle activity of TA (at I1 and I2) and PL (at I1) decreased as the stimulation site changed from 1 to 4 but increased in proportion to the intensity. In contrast there was an increase of muscle activity at I1 and I2 as the stimulation site changed from 1 to 4 in GA, RF and BF in S1.

The muscles GA, RF and BF were co-activated only at I1 and I2 for site 1 in S2. Moreover there was an increase of TA and PL at I3. At site 2 the co-activation changed from GA, RF and BF at I1 to TA, GA and BF at I3. The muscle activations at site 3 and site 4 compared to site 1 and site 2 was low at I1. An increase of muscle activity at site 3 and site 4 occurred when the intensity was above the PTh i.e. I2 and I3.

The results indicated that site 1 is different from other the sites due to the co-activation of TA and PL shown as a bell shape. In comparison, site 4 showed the co-activation of GA, RF and BF. There is a distinct time activation between S1 and S2 for site 1 compared to the other sites, where no distinct activation coefficient shapes were identified.

IV. Discussion

The movements of each muscle in NWR could not be quantified by the net result of the muscle activations since the EMG data was normalised. This means that the contribution of each muscle in $\mathbf{W}$ should be considered as relative weightings and not absolute, since each subjects could have different normalisation coefficients for each muscle. Normalisation makes the data comparable between subjects with the disadvantage of reducing the reflex amplitude of the muscles.

In most of the cases, high activity in one synergy activation coefficient corresponds to low activity in the other one at a particular timepoint. The results of $\mathbf{W}$ and $\mathbf{C}$ for a particular site and intensity are related. In S1 the high $\mathbf{W}$ value of TA and PL was reflected on the corresponding $\mathbf{C}$. This is due to their average waveforms being similar in shape, causing the sum of these activations to be a distinct feature which could be the reason for the for the high $\mathbf{C}$ values in site 1 for S1. In S2 the high $\mathbf{W}$ value of GA, RF and BF was reflected on the corresponding $\mathbf{C}$.

Site 4 shows that the co-activation of GA, RF and BF had incomplete $\mathbf{C}$ shapes compared to the generic bell shape. The reason for this could be the fact that the upper limit of the reflex window was limited to 150 ms and that RF and BF possibly had later reflexes than 150 ms. The chosen reflex window ranged from 80-150 ms post-stimulus in order to extract reflexes since voluntary movements were undesirable [19].

The contribution of each muscle synergy were site dependent. This could be seen in the increasing activity of PL at site 3, as this muscle contribution could possibly be related to the eversion movement of the foot. TA in S1 at site 3 and site 4 was noticeably lower than at site 1 and site 2. This could possibly be related to the stimulation being near the heel and therefore lead to plantar flexion as it was reflected in the high activity of GA.

Due to the extracted muscle synergies being time-invariant it was not possible to detect how the muscle activity of each muscle within a muscle synergy shifted over time. In future studies a extraction of time-varying muscle synergies could be relevant in order to quantify how the muscle activity shifts in time and achieve a dynamic quantification.

V. Conclusion

This study showed that the extraction of time-invariant muscles synergies from the NWR of 11 subjects were successfully conducted using NMF. The investigation indicated that increasing the stimulation intensity would increase the muscle contribution in S1 and S2. Furthermore, the change of stimulation site from 1 to 4 altered the muscle activity pattern from a co-activation of TA and PL to GA, RF and BF in S1. Intensity dependency was indicated as the muscle contribution at site 3 and site 4 in S2 first became noticeable at intensities above the PTh.

ACKNOWLEDGMENT

The authors would like to thank the subjects who participated in the study and our supervisor Ole K. Andersen and co-supervisor Fabricio A. Jure. A thank you to Jan Stavnshoej for technical support.

References

[1] K. E. Hagbarth, "Spinal withdrawal reflexes in the human lower limbs," *Journal of Neurology, Neurosurgery & Psychiatry*, vol. 23, no. 3, p. 222, 1960.

[2] O. K. Andersen, E. G. Spaich, P. Madeleine, and L. Arendt-Nielsen, "Gradual enlargement of human withdrawal reflex receptive fields following repetitive painful stimulation," *Brain Research*, vol. 1042, no. 2, 2005.

[3] T. Wojtara, F. Alnajjar, S. Shimoda, and H. Kimura, "Voluntary and Reflex Muscle Synergies in Upper Limbs," *Biosystems & Biorobotics*, vol. 1, pp. 575–580, 2013.

[4] G. Torres-Oviedo, J. M. Macpherson, and L. H. Ting, "Muscle synergy organization is robust across a variety of postural perturbations," *Journal of neurophysiology*, vol. 96, no. 3, pp. 1530–46, 2006.

[5] T. Wojtara, F. Alnajjar, S. Shimoda, and H. Kimura, "Muscle synergy stability and human balance maintenance," *Journal of NeuroEngineering and Rehabilitation*, vol. 11, p. 129, 2014.

[6] M. C. Tresch and A. Jarc, "The case for and against muscle synergies," *Current Opinion in Neurobiology*, vol. 19, no. 6, pp. 601–607, 2009.

[7] K. Shima and T. Tsuji, "Classification of combined motions in human joints through learning of individual motions based on muscle synergy theory," *IEEE/SICE International Symposium on System Integration*, pp. 323–328, 2010.

[8] L. H. Ting and L. J. Mckay, "Neuromechanics of muscle synergies for posture and movement," *Current Opinion in Neurobiology*, vol. 17, no. 6.

[9] A. D'Avella, A. Portone, L. Fernandez, and F. Lacquaniti, "Control of fast-reaching movements by muscle synergy combinations, journal = The Journal of Neuroscience," vol. 26, no. 30, pp. 7791–810, 2006.

[10] M. C. Tresch, P. Saltiel, and E. Bizzi, "The construction of movement by the spinal cord," *Nature Neuroscience*, vol. 2, no. 2.

[11] J. A. B. Manresa, M. B. Jensen, and O. K. Andersen, "Introducing the reflex probability maps in the quantification of nociceptive withdrawal reflex receptive fields in humans," *Journal of Electromyography and Kinesiology*, vol. 21, no. 1, pp. 67–76, 2011.

[12] D. D. Lee and H. S. Seung, "Algorithms for Non-negative Matrix Factorization," *Neural Information Processing Systems*, vol. 13, pp. 556–562, 2001.

[13] J. Frre and F. Hug, "Between-subject variability ofmuscle synergies during a complex motor skill," *Frontiers in Computational Neuroscience*, vol. 6, 2012.

[14] M. B. Jensen, J. Biurrun, and O. K. Andersen, "A new objective method for acquisition and quantification of reflex receptive fields," *Pain*, vol. 156, no. 3, pp. 555–64, 2015.

[15] M. B. Jensen, J. A. B. Manresa, K. S. Frahm, and O. K. Andersen, "Analysis of muscle fiber conduction velocity enables reliable detection of surface EMG crosstalk during detection of nociceptive withdrawal reflexes," *BMC neuroscience*, vol. 14, p. 39, 2013.

[16] M. W. Berry, M. Brown, A. N. Langville, V. P. Pauca, and R. J. Plemmons, "Algorithms and Applications for Approximate Nonnegative Matrix Factorization," *Computational Statistics and Data Analysis*, vol. 52, no. 1, p. 155173, 2007.

[17] M. S. Shourijeh, T. E. Flaxman, and D. L. Benoit, "On Running Non-Negative Matrix Factorization On Individual Participants for Muscle Synergies Extraction," *Conference: CSCBCE/IEEE EMBS*, 2014.

[18] T. Burkholder and K. Antwerp, "Practical limits on muscle synergy identification by non-negative matrix factorization in systems with mechanical constraints," *Medical & Biological Engineering & Computing*, vol. 51, no. 1, pp. 187–196, 2013.

[19] J. L. Rhudy, C. R. France, and S. McGlone, "Using normalized EMG to define the nociceptive flexion reflex (NFR) threshold: Further evaluation of standardized NFR scoring criteria," *Pain*, vol. 145, no. 1-2, p. 211218, 2009.

The Extraction of Time-Invariant Muscle Synergies in the Nociceptive Withdrawal Reflex in the Lower Limb

Barak El-Omar, Ardalan A. Wais, Navinder S. Dhillon & Alari Varmann
Group 7405

1st semester Biomedical Engineering and Informatics
20th December 2016

AALBORG UNIVERSITY
STUDENT REPORT

Table of Contents

Background 1

The purpose of this chapter is to provide the necessary background knowledge in order to understand the mechanisms and neurophysiology involved in the nociceptive withdrawal reflex (NWR). Section 1.1 introduces nociception which is the nervous system response to noxious stimulus.

Section 1.2 introduces the NWR and the neuronal pathway from sensory stimulation to motor response. A distinguishing between the ipsilateral reflex and crossed extensor reflex is made. The NWR is further elaborated upon in section 1.3 in terms of introducing the concept of reflex receptive fields (RRF) which are sensory areas which can elicit a NWR response when stimulated.

Section 1.4 introduces the concept of muscle synergies which is defined as the collaboration between different muscles in order to perform a particular motor task and how these muscle synergies can be decomposed and analysed using non-negative matrix factorization.

1.1 Nociception

In this section the nociceptors referred to are those present in the cutaneous layer, and the stimulation thresholds described relates to electrical stimulation. The cell bodies of nociceptors are located mainly in the dorsal root ganglia. [Purves et al., 2012]

Nociceptors are a specific type of primary sensory neurons with free nerve endings that respond to various types of noxious stimuli [Loeser and Treede, 2008]. Stimulus of any modality can be considered potentially damaging noxious by the nervous system once the its intensity exceeds a specific threshold that depends on the sensitivity of the neuron's receptive field. [Loeser and Treede, 2008] Polymodal nociceptors are primary sensory neurons that respond to multiple types of noxious stimuli, while unimodal nociceptors respond to only one type of noxious stimulus, see table 1.1. [Purves et al., 2012]

There are three different types of sensory fibers which are responsible for transmitting a particular type of information to the spinal dorsal horn (SDH). (1) The A-β fibers are thick in diameter and myelinated which result in these fibers having high conduction velocity, low stimulation threshold and they transmit sensory information of light touch to the SDH. (2) The A-δ fibers are less myelinated and thereby have a smaller conduction velocity compared to the A-β fibers. Furthermore, A-δ fibers respond to thermal and mechanical stimuli and have a higher stimulation threshold compared to A-β fibers. (3) The third type of sensory fibers are the C fibers. These are not myelinated and thereby have the slowest conduction velocity type of sensory fibers. They have the highest stimulation threshold. [D'Mello and Dickenson, 2008]

Stimulation of the nociceptors result in the noxious information being transmitted to the SDH. Further processing takes place in different laminae of the SDH depending on the intensity and modality of the signal. Within these laminae are the nociceptive specific cells which receive information of noxious stimuli. Also present in SDH are the wide dynamic range neurons which receive information about touch as well as noxious stimuli. Table 1.1 provides an overview of the different types of sensory fibers and their characteristics [D'Mello and Dickenson, 2008]

Table 1.1. Overview of the different types of sensory fibers, their connection in SDH and characteristics with regard to conductivity and activation. The comparison of the nociception conveying fibers, relate to electrical stimulation. Based on information from the article D'Mello and Dickenson [2008].

Type	Response to stimuli	Myelination	Conduction velocity	Stimulation threshold
Aβ-fiber	Light touch	Myelinated	High conduction velocity	Low stimulation threshold
Aδ-fiber	Thermal and mechanical	Less myelinated	Medium conduction velocity	Medium stimulation threshold
C-fiber	Thermal, mechanical and chemical	Non-myelinated	Low conduction velocity	High stimulation threshold

1.2 Nociceptive Withdrawal Reflex

Eliciting a NWR results in a contraction of certain muscles as well as inhibition of the antagonistic muscles (reciprocal inhibition). When a noxious stimulus is elicited for instance, under the sole of the foot, the A-δ and C fibers transmit the action potential to SDH through an afferent pathway [D'Mello and Dickenson, 2008]. This results in the activation of the inhibitory interneurons in SDH which are connected to the ventral horn. The activation of the inhibitory interneurons results in inhibition of antagonistic muscle contraction during stimulus. For instance as the antagonistic muscle gastrocnemius is inhibited the excitatory interneurons stimulate motor neurons in the anterior grey horns and cause the agonist muscle, for instance, tibialis anterior to contract. There are different types of reflexes which can occur by similar stimulus, but the reflex reaction is posture dependent. The following describes the crossed extensor reflex and the ipsilateral reflex. [Martini et al., 2014]

Crossed Extensor Reflex Arc

Contralateral arc or crossed extensor reflex refers to the sensory stimulus causing the motor response to occur on the opposite side of the stimulated limb. Both the crossed extensor and the NWR occur simultaneously e.g. stepping on a needle with the right foot and causing the NWR to remove the foot away from the surface, while the crossed extensor reflex supports the body by straightening the left leg. [Martini et al., 2014]. A crossed extensor reflex involves the crossing of the nociceptive response gained from the axons of interneurons to the other side of the spinal cord. Stimulation of the motor neurons that control the extensor muscles of the unharmed leg results in straightening of the leg to support the shifting weight. [Martini et al., 2014]

Ipsilateral Reflex Arc

The ipsilateral reflex arc refers to the sensory stimulus and the motor response that occurs on the same side of the body e.g. stepping on a needle with the right foot while seated

leading to contraction in the TA to withdraw the limb from the needle [Martini et al., 2014]

1.3 Reflex Receptive Fields

Elicitation of reflexes by electrically stimulating the cutaneous layer of the foot has been investigated by Grimby [1963] with the purpose of providing an understanding of the withdrawal reflexes. Stimulation of an area on the cutaneous layer above a certain threshold will elicit a reflex response. These areas are termed reflex receptive field (RRF). The involvement of the RRF have shown to have an important part in studies of the NWR as every muscle has their own cutaneous RRF. Stimulation of RRF results in a reflex response that causes the limb to withdraw from the stimulus. [Andersen et al., 2005] Since multiple muscles have overlapping RRF it implies that the reflex movement is a net result of the activated muscles which are overlapping in the RRF, see figure 1.1. Furthermore each RRF has their own reflex boundary, where the sensitivity of the RRF is high in the center and gradually decreases with increasing distance from the center. [Andersen et al., 2005]

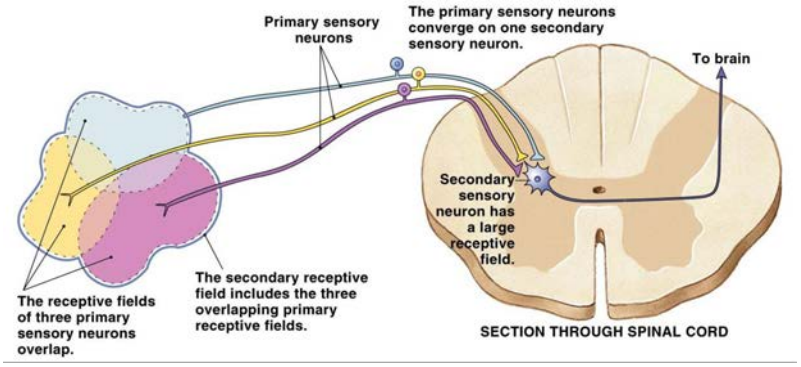

Figure 1.1. Three overlapping reflex receptive fields (yellow, blue, purple) which transmits the information to a receptive cell in the SDH. From here the signal is processed in the brain. [Austin-Community College, 2016]

The gradual sensitivity change from RRF center results in an increasing time delay in the reflex response. Moreover this implies that elicitation of a reflex from the RRF boundary requires a stronger stimulus. The closer the stimulation occurs to the boundary the longer the time delay. The RRF boundary can be expanded by repetitive stimulation at a specific site. [Andersen et al., 2005] The NWR has been shown to be posture dependent as well as intensity dependent. In addition the actual motor output might vary considerably among subjects [Martini et al., 2014; Andersen et al., 2005]

1.4 Muscle Synergies

One of the relevant parameters to understand in the muscle performance for any joint or joint complex is the muscle coordination. Coordinated activity of muscle groups driven by a single neural command signal towards a common goal defines a muscle synergy hence it is critical to clarify the goal and the time span in which the muscle groups collaborate to identify these synergies. [Bronzino, 2000; Winter, 2009; Torres-Oviedo et al., 2006;

D'Avella, 2016] Muscle synergies have a group of features shared by a series of muscle patterns making it possible to construct a low-dimensional representation of the motor output. These features can be specified in the spatial domain, which is the balance of activations across the muscles, and in the temporal domain [D'Avella, 2016; Tresch and Jarc, 2009]. A muscle synergy can be expressed as a D-dimensional vector $\boldsymbol{W}$ of weighting coefficients by representing a group of D muscles. The activation balance among the muscles is specified by the weighting coefficients in $\boldsymbol{W}$. Scaling in amplitude the entire vector $\boldsymbol{W}$ can cause different levels of activation to be generated by a single muscle synergy. [D'Avella, 2016; D'Avella et al., 2003] This gives the following equation:

$$\mathbf{M} = \mathbf{W}C \tag{1.1}$$

where C is a scaling coefficient and $\boldsymbol{M}$ is the pattern of muscle activation i.e. the recruitment level of each muscle. Many distinctive muscle activation patterns can be generated by a group of N synergies, $\{\mathbf{W_i}\}_{i=1,..,N}$, and this yields the following equation [D'Avella, 2016; D'Avella et al., 2003]

$$\mathbf{M} = \mathbf{W}_1C_1 + \mathbf{W}_2C_2 + \cdots + \mathbf{W}_NC_N = \sum_{i=1}^{N} \mathbf{W}_iC_i \tag{1.2}$$

In the temporal domain, an either time-invariant or time-varying muscle synergy could be found, as some muscle activation vectors are time-dependent. A muscle synergy is time-invariant if a balance of muscle activation is the same at all times. [D'Avella, 2016] Equation (1.2) can be written, taking time into account, as following if all the muscle synergies are time-invariant:

$$\mathbf{M}(t) = \sum_{i=1}^{N} \mathbf{W}_iC_i(t) \tag{1.3}$$

where both the scaling coefficient for the i-th muscle synergy, *C(t)* and the muscle activation, $\boldsymbol{M}(\mathbf{t})$, are at a time t. The muscle waveforms related to each muscle synergy are synchronous since the waveform of the different muscles is the same $C_i(t)$ waveform, i.e. if a muscle synergy is activated at a time t, all muscles within that muscle synergy are active allowing no temporal delay. A time-varying muscle synergy is not necessarily synchronous because of the collection of different waveforms, each one specific for a muscle, which allows for delays between muscles within the same muscle synergy. [D'Avella, 2016; Tresch and Jarc, 2009; D'Avella et al., 2003] A time-varying muscle synergy vector, $\boldsymbol{W}(\mathbf{t})$, and equation (1.2) express these waveforms

$$\mathbf{M}(t) = \sum_{i=1}^{N} \mathbf{W}_i(t - t_i)C_i \tag{1.4}$$

where the equation includes one time delay, t_i, and one scaling coefficient, C_i, for each muscle synergy. The temporal structure of the muscle synergies and their relative delays leads to the capturing of the time dependence of the muscle activation waveforms. In this case, the motor output is represented parsimoniously by the time-varying muscle synergies since a few delay and scaling coefficients are adequate to identify numerous muscle patterns in muscle synergies. [D'Avella, 2016]

Generation and Recording of Muscle Activity Related to Nociceptive Withdrawal Reflex

2

Electrical stimulation is often used to elicit a NWR by using non-invasive electrical stimulation within the RRF where the intensity of the stimuli is not painful or damaging to the skin. Electrical stimulation is more preferred than for instance mechanical or heat stimulation, because of the required intensity to elicit a NWR. In order to elicit a NWR with heat stimulation the intensity of the heat stimuli has to be high, and high-intensity stimuli may cause damage to the skin. The number of repetitions is limited in heat stimulation since consecutive repetitions may cause damage to the skin too. Furthermore, the analysis and interpretation of the elicited responses may be complicated due to the variation in heat transduction with varying skin thickness [Andersen et al., 1999].

2.1 Elicitation of Nociceptive Withdrawal Reflex

Electrical stimulation can consist of trains of stimuli. A train consists of one or more bursts with a certain burst frequency. A burst contains a number of pulses with a pulse interval and a pulse frequency. A pulse has an amplitude and a pulse width. [Doucet et al., 2012; Birkill et al., NA]

A stimulation with the lowest amount of ampere per elicitation of the reflex and least amount of pulses is defined as an optimal stimulation. The study Tørring et al. [1981] has found that in order to obtain a NWR in the TA muscle the pulse width should not exceed 1 ms. Increasing the pulse width over 1 ms causes no change to the threshold of the reflex, but decreasing the pulse width triggers a precipitous increase of the threshold. In addition, the optimal pulse interval is at 1 ms or more, since the threshold of the reflex is increased when the pulse interval is below 1 ms. A train consisting by one burst that contains five pulses were found most effective in terms of eliciting the NWR. To implement a unipolar stimulation that fulfills the above-described criteria, one train consisting of one burst, five pulses, 1 ms pulse width and pulse intervals between 2-5 ms, leads to a stimulation with a frequency between 200 and 500 Hz. [Tørring et al., 1981]

Stimulation Site and Methods

The elicitation of NWR is based on activating the muscles through electrical stimulation with negative electrical pulses so that the most efficient propagation of stimulus is attained. In addition the cathodes of the stimulator should therefore be placed proximal to the desired stimulation site. [Birkill et al., NA] The cathode needs an anode for the stimulus to be perceived at the stimulation site. An anode is preferably large in order for it to be used as a common anode for numerous cathodes. [Jensen et al., 2015]

The electrical stimulation can be trans- or percutaneous. These stimulation methods involve different electrodes for stimulation. The transcutaneous stimulation uses surface electrodes placed on the skin area that is desired to be stimulated. The percutaneous stimulation uses invasive electrodes that is inserted into a muscle to achieve stimulation on the nerve bundle. Since transcutaneous stimulation is site-selective, it is more preferable to use this stimulation method to elicit NWR responses. [Doucet et al., 2012]

Nociceptive Withdrawal Reflex Threshold

A NWR threshold is determined by the intensity of stimulation needed to elicit the NWR. Research has shown that the NWR threshold is often highly correlated with the pain threshold and also that the magnitude of the reflex response is related to the intensity of pain perception. [Rhudy and France, 2007] In addition, other factors as diurnal rhythms, activity of baroreceptors, attention and awareness to stimuli as well as stimulation site affects the NWR threshold [Bjerre et al., 2011; Skljarevski and Ramadan, 2002].

The reflex window is defined as 70-200 ms after stimulation onset is where the EMG activity reflects a reflex. EMG activity above 20 μV in the reflex window defines a reflex and the intensity of the reflex threshold is defined as the lowest intensity that elicits a reflex response in three sequential stimulations.[Rhudy and France, 2007; Bjerre et al., 2011] A study by Rhudy and France [2007] has found that the most accurate, stable and reliable methods with regard to scoring criteria for the EMG is the interval peak z score and the interval z score. The cut-points for the threshold definition have to be taken into account since they may need to be adjusted according to research design [Rhudy and France, 2007]. The NWR threshold is defined as a specific z score value in case of the z score criteria. Studies have defined a z score of 12 for the reflexes for TA which means that when a z score is less than 12 no reflex is present while a z score over 12 means that a reflex is present with a probability above 50 %. The z score is used to find the electrical intensity when a NWR is elicited which becomes a measure of the reflex threshold. This method is objective since no subjective pain ratings are used which is why this reflex method is preferred when studying the RRF. [Jensen et al., 2015]

Habituation and Startle Reflex

The use of different types of stimulation including electrical stimulation with a fixed intensity and site may lead to habituation which is seen in experiments involving NWR. Habituation is when a repeating stimulus causes an organism to decrease or cease the stimulus response. To minimize the habituation of the reflexes the simulation intensities should be above the reflex threshold and lower than twice the reflex threshold. In addition,

the habituation effect can be minimized by blinding the subjects to timing and stimulus site and randomizing the sessions. [Bjerre et al., 2011]

Besides habituation there is a startle reflex which is elicited by any sudden stimuli that has a rapid onset. The startle reflex can be elicited by electrical stimulation and the latencies of the startle reflex response and the NWR response in the limb muscles overlap. This makes the startle reflex a possible artifact along with habituation when studying the NWR. The startle reflex occurrence can be minimized with repeated presentation to stimulus and with short inter-stimulus intervals (ISI). The occurrence of the startle reflex can be eliminated by using a short ISI and repeated innocuous stimuli at different levels prior to the recordings of the NWR. [Dowman, 1992]

2.2 Electromyography

The electrical activity in muscles is generated by the firing of several motor units. A motor unit consists of a motor neuron and the muscle fiber(s) it stimulates. A firing motor unit discharges action potentials named motor unit action potentials (MUAP). The size and shape of MUAP is dependent on the muscle fiber types and intensity of contraction.

When an action potential reaches the axon terminal of the motor unit the release of acethylcoline (ACh) from the vesicles is triggered. This leads to a cascade of reaction resulting in a muscle contraction (see appendix A). The action potential can be detected and recorded using surface electromyography (EMG).[Martini et al., 2014] The EMG signal itself is superposed from the activity of motor units where the amplitude of the signal reflects the level of muscle contraction, this is illustrated in figure 2.1 [Konrad, 2006].

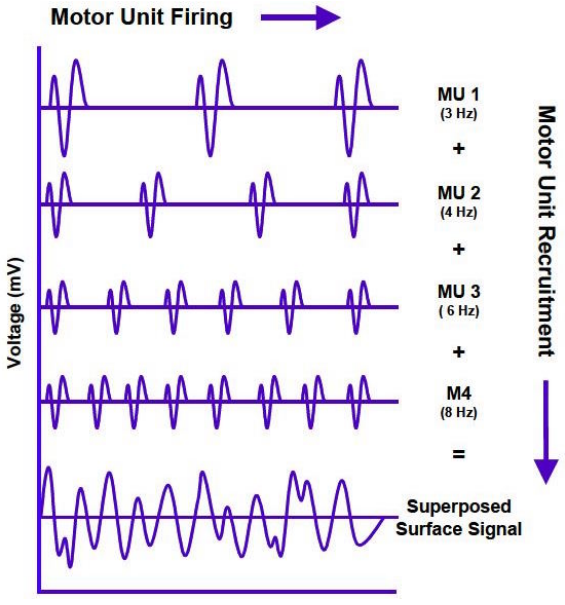

Figure 2.1. Firing frequency of different motor neurons (MU) from MU1 to MU4. Each MU has their own frequency signal amplitude. The bottom signal is the superposed signal of the four MU's. [Konrad, 2006]

For surface EMG, the amplitude ranges between ± 5 mV and the frequency of EMG ranges

from 6 to 500 Hz but frequency power is mainly found between 10 to 250 Hz [Konrad, 2006]. EMG can be detected using different types of configuration where recording of dynamic action and movement is typically performed using the single-differential electrode configuration [Konrad, 2006].

2.3 Amplification

The following sections explains the use of single-differential and double-differential amplification in order to gain perspective of usages, advantages and disadvantages of the different configurations.

Single-Differential Amplification

Due to the small amplitude of the EMG signal it is pre-amplified using a differential amplifier for it to be properly visualized as illustrated on figure 2.2 [Konrad, 2006].

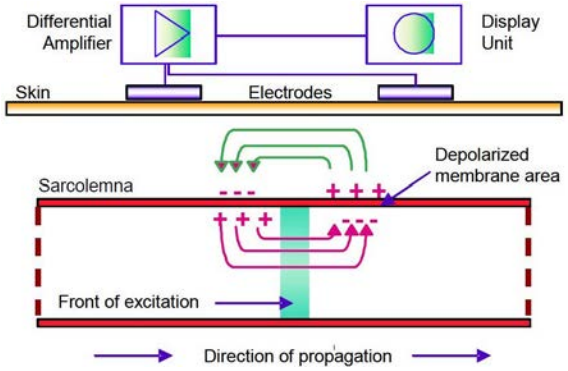

Figure 2.2. Depolarization of membrane in the sarcolemma with the action potential travelling in the direction of propagation. The electrodes placed on the skin measures the difference in potential which is then amplified and visualized. [Konrad, 2006]

On figure 2.3 it is shown how the action potential travels and the potential difference changes as it reaches and leaves the electrodes.

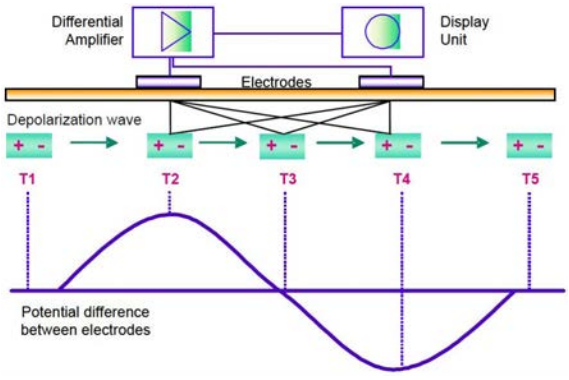

Figure 2.3. Generated action potential propagates in the direction of the electrodes. At time point T1 the action potential is generated. At T2 it steadily increases and the difference is positive. At T3 the distance of the action potential from the electrodes is equal resulting in a potential difference of zero. At T4 the potential difference is below zero as the action potential is closer to 2nd electrode. [Konrad, 2006]

At time point, T1 an action potential is generated and begins to travel towards the electrodes. As the action potential reaches the first electrode, T2, the potential difference is positive since the distance to the first electrode is the shortest. At T3 the potential difference is zero because the action potential has an equal distance to both electrodes. At T4 the action potential has the shortest distance to the second electrode and the potential difference goes below zero. [Konrad, 2006]

The single-differential amplifier finds the difference between the signals acquired from the electrodes. This leads to the elimination of common-mode signals, which is noise appearing at each terminal with equal amplitude and phase. The measure of how well the common-mode signals have been eliminated is given by the common-mode rejection ratio (CMRR). The CMRR is calculated by finding the relationship between the common-mode and the gain in the differential amplifier. The CMRR should be as high as possible and ideally infinite. [Winter, 2009] A CMRR of minimum 95 dB is preferred [Konrad, 2006].

Double-Differential Amplification

When measuring a muscle with the EMG method, the activity from nearby muscles can potentially be acquired in the same EMG signal. The activity from nearby muscles are unwanted and are not eliminated with the single-differential amplifier, which can be eliminated by using a double-differential amplifier. The double-differential amplifier consists of three measurement electrodes from the surface of the skin, which is illustrated on figure 2.4. Two signals are acquired from respectively electrode one and two and electrode two and three. These to signals are then undergoing two separately levels of differentiation where the outcome of these two are one single differential EMG signal. [Luca, 1997]

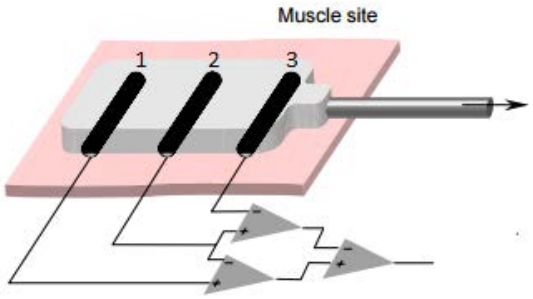

Figure 2.4. Illustrates the setup and circuit for a double-differential amplifier. Two signals are measured from electrode one and two and electrode two and three.[Delsys, 2003]

The double differential amplifier is specifically designed to reduce the muscle activity from the adjacent muscles.

Filtering

The EMG recording should not use any hardware filters except the anti-aliasing filter. A band pass is filter is preferred for further filtering [Konrad, 2006]. With regard to choosing

the cut-off frequency for the high pass, the decision should be made based on which muscles the EMG is recorded on along with whether the activity measured is isometric or dynamic but as a rule of thumb a high-pass cut-off frequency of 10 Hz and low-Pass frequency of 250 Hz can be used as the main frequency power is found in this frequency range. [Konrad, 2006]

Noise Factors

The characteristics of an EMG signal can be influenced by different factors during the recording process. These factors can result in unwanted noise appearing in the signal. The following are different noise factors which influence the EMG signal. (1) External noise is the most influential noise factor when recording an EMG signal. It is also the most demanding with regard to removal when recording an EMG signal. External noise is caused by power-lines and other electrical equipment in the recording environment as well as poorly grounded equipment. (2) Dependent on the recording site and individuality among subjects, issues related to conductivity in the tissue can occur. Influences such as thickness of the outer cutaneous layers, temperature, volume of adipose tissue all affects the overall conductivity during the recording. [Konrad, 2006]

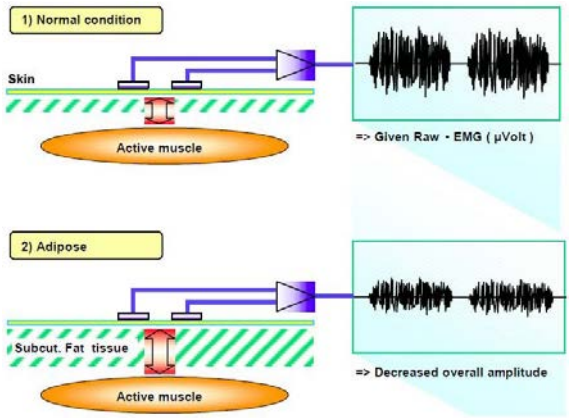

Figure 2.5. Influence of tissue thickness and skin-to-muscle distance on the EMG signal. 1) Short skin-to-muscle distance and thin subcutaneous layer resulting in high conductivity and clear amplitude of the signal. 2) Long skin-to-muscle distance and thick subcutaneous layer resulting in lower conductivity and smaller amplitude of the signal. [Konrad, 2006]

Figure 2.5 exemplifies how the thickness of tissue might impact the recording: 1) Shows good conductivity the subcutaneous layer is thin and the skin-to-muscle distance small resulting in a high EMG amplitude. 2) shows that the subcutaneous layer is thick which lowers the conductivity. Furthermore, the skin-to-muscle distance is large causing a decrease in the amplitude of the EMG signal. [Konrad, 2006] (3) Movement artifacts typically appears when recording dynamic movement. This is due to cables not being sufficiently secured which can cause the electrodes to detach from the recording site. In order to secure the electrodes, it is suggested to tape the wires but not the electrodes themselves as is would lead to different amount of electrode-to-skin tension. [Konrad, 2006] (4) Cross-talk which is the contribution of EMG from muscles adjacent to the recording site. Cross-talk can contribute between 10 % to 15 % of the overall content of

the signal when present. [Konrad, 2006] Electrode size and inter-electrode distance should especially be taken into consideration if muscles adjacent to the recording site are close. Smaller electrodes allow for better accuracy when selecting recording site and smaller inter-electrode distance as well which can decrease the influence of cross-talk. The disadvantage however that smaller electrodes results in higher impedance making the recording more difficult. [Konrad, 2006]

Project Aim 3

Studies have identified muscle synergies in voluntary movements but it has not been investigated in the involuntary movement. The NWR can be elicited in the lower limb by delivering electrical stimulation under the sole of the human foot. The EMG recordings of the following five muscles: tibialis anterior (TA), gastrocnemius medialis (GA), peroneus longus (PL), rectus femoris (RF) and biceps femoris (BF). Based on this, the aim of the present study was to investigate the contribution of muscle synergies in the NWR and how this is affected by varying stimulus intensity and stimulation site.

Methodology 4

In this chapter the characteristics of the subjects for the experiment is defined. Furthermore the experimental set-up is described including the three parts of the experimental session. Finally the methods for acquiring data is described. In this part the different electrode types and usages are explained along with electrode placement and the signal acquisition.

4.1 Subjects

This study included 11 healthy subjects. A suitable subject is in this study defined by not having any of the following conditions:

- Neurological diseases
- Injured right leg
- Metallic implants
- Diabetes
- Pregnancy

Individuals with diabetes were excluded from the study since there is a risk of having an increased cortisol level. Cortisol is the stress hormone which is commonly the reason for a higher sympathetic activity and is often seen in individuals with diabetes. Having a higher sympathetic activity results in an increased heart rate and can potentially have an influence on the behaviour. [Chiodini et al., 2007]

Pregnant women are also excluded as the structure of their feet changes during pregnancy. They gradually lose the height of the arch which can lead to subjects with painful musculoskeletal conditions and failing mechanics. [Segal et al., 2013]

The healthy subjects had an age between 21 and 24 years and consisted of five men and six women. They were asked to refrain from alcohol, caffeine and drugs at least 2 hours prior to the experiment as it is suspected that stimulants of any sorts might affect the NWR response. Performing strenuous leg exercise was not permitted for 24 hours prior to the experiment in order to insure that muscle fatigue would not be affect the NWR response.

4.2 Experimental set-up

The subject was seated on the bed and the legs resting comfortably with a bending of 35°. The TA, GA, PL, RF, and BF muscle were identified on the right leg in order to prepare the EMG electrode positioning. The electrode positions were prepared by shaving

leg hair, scraping the outer cutaneous layer with a foot file and cleansing with isopropyl alcohol before the electrodes were mounted on the leg. Three electrodes were placed in a line parallel to the muscle belly on the TA, GA, PL and RF. TA, GA and PL are adjacent to one another meaning the risk of cross-talk between these muscles is high. In order to reduce the cross-talk they were measured by using double-differential amplifiers. Only two electrodes were placed on the BF. Cross-talk between BF muscle and any other muscle was not suspected.

The interelectrode distance between the three electrodes was approximately 20 mm (center-to-center). The reference electrode for each set of electrodes per muscle were combined into a common reference placed on the lateral malleolus of the right leg. For the stimulating electrodes the sole of the right foot was scraped with a foot file and cleansed with isopropyl alcohol whereafter four cathodes was mounted. The dorsum of the right foot was also scraped with a foot file and cleansed with isopropyl alcohol before mounting the common anode.

A custom-made software, Mr. Kick v. 2.9230, made by Knud Larsen, SMI, Aalborg University, was used in this study to acquire the data. The software was used to first set up the gain or sensitivity on the EMG amplifiers to ensure the full range of the ADC was used without saturating the EMG signal. Therefore the subject was asked to contract each of the five muscles one at a time in order to adjust the gain or sensitivity for each muscle before starting the session. The experimental session was divided into three parts: (1) familiarization, (2) pain threshold determination and (3) recording of NWR responses.

In the first part the subject was introduced to the sensation of the electrical stimulation. The subject was stimulated at a low intensity at each stimulation site. Stimulation electrodes were moved slightly if the subject felt a sensation of the stimuli radiating caused by direct nerve trunk stimulation. The session carried on when the subject was familiarized with the sensation.

In the second part the NWR threshold (NWR-T) was determined using the up-down staircase method. It was assessed that a z score higher than 12 was a reflex. This z score was used for all muscles. The subject was stimulated with a starting intensity at 1 mA and then increased with a step of 2 mA until a NWR was detected. Then the intensity decreased with a step of 1 mA until a NWR was not detectable. Thereafter a set of three ascending and descending estimations of the NWR-T was achieved by increasing and decreasing with a step of 0.5 mA. The mean of the last two ascending and descending estimations was calculated and resulted in the final NWR-T for the subject. Afterwards the pain threshold was determined. In order to determine the pain threshold the subject was stimulated at site 1 with a starting intensity based on the NWR-threshold and then manually increased by 2 mA with a stimulus interval between 3-5 s. The pain threshold for the site was determined by a subjective assessment from the subject. The pain thresholds for the remaining sites were found in a random order. Gradual adaptation at these sites was avoided by intermittently stimulating site 1 at the detected pain threshold level.

The third part consisted of recording the NWR responses from the subjects. Nine stimulation at each site for each intensity resulted in 108 stimulations per subject. The stimulations were given in three rounds of 36 stimulations with a break of 2 minutes

between each round and were given in a random stimulation site order. The three intensities that were used are 0.7x, 1.1x and 1.7x times the pain threshold at each stimulation site.

4.3 Signal acquisition

For the EMG signal acquisition three electrodes per muscle of the type 720, AMBU A/S were positioned according to the SENIAM guidelines on the belly of the muscles [SENIAM, 2016] and a common reference electrode, placed on the lateral malleolus, of the same electrode type was used. The placements of the recording electrodes are illustrated on figure 4.1 (a) and (b).

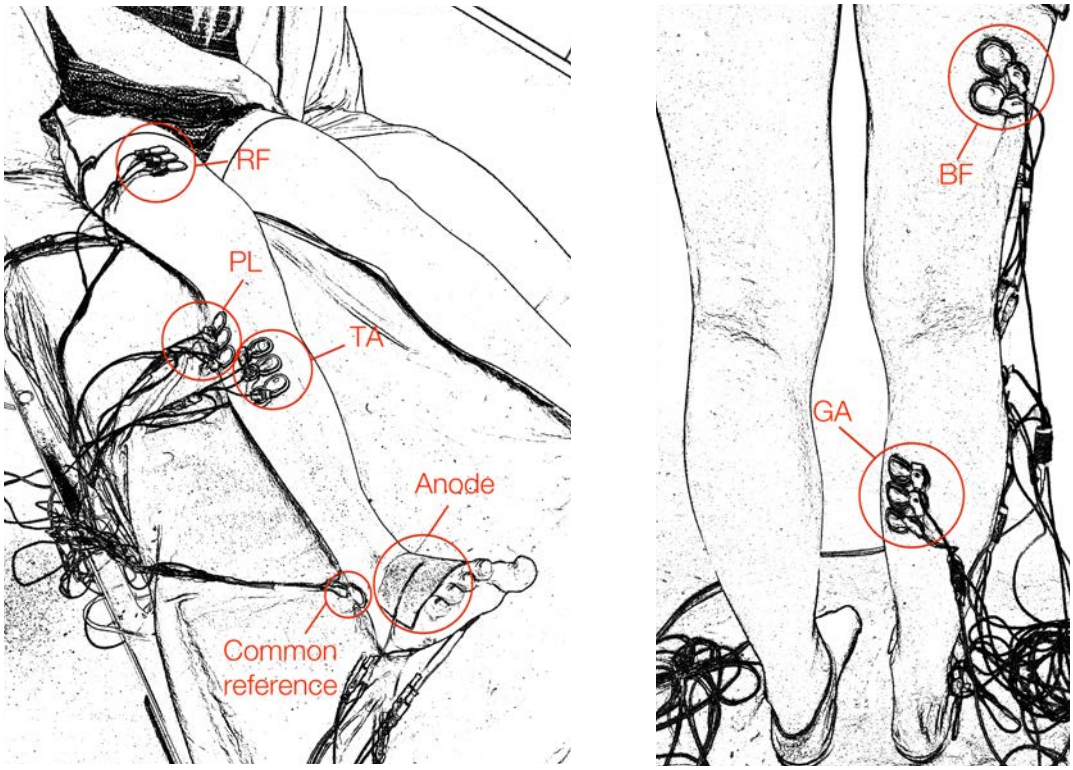

(a) (b)

Figure 4.1. The placements of the recording electrodes of TA, PL, RF and the common reference in (a), BF and GA in (b)

Four cathodes (surface stimulation electrodes) (type 700, AMBU A/S) were positioned non-uniformly under the sole of the foot. An anode (PALS; Axelgaard, Fallbrook, CA) was placed on the dorsum of the foot as to ensure the stimulus would be perceived coming from the sole of the foot, see figure 4.2. Each electrical stimulus consisted of a constant current pulse train consisting of five individual 1 ms pulses which was delivered at 200 Hz by an electrical stimulator (NoxiTest IES 230; Aalborg, Denmark). The ISI was set to be between 5-8 s.

The EMG signals for the TA, GA, PL and RF were pre-amplified using a double-differential amplifier and BF using single-differential amplifier. All EMG signals were filtered with a 2nd order high and low pass filter. The passband ranged from 5 Hz to 500 Hz and the

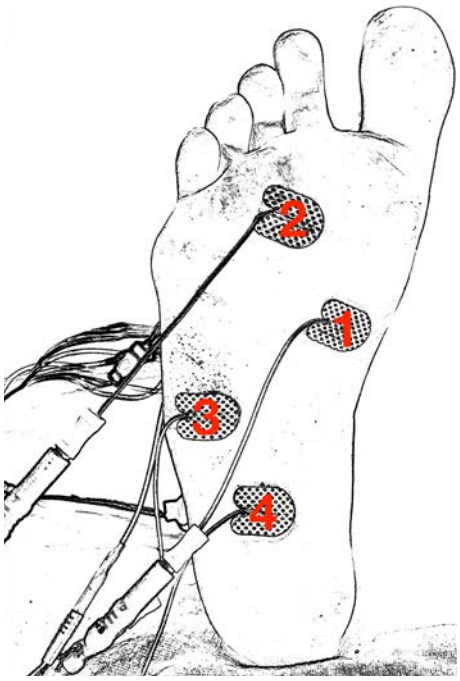

Figure 4.2. The placements of the stimulation electrodes

EMG signals were recorded with a sampling frequency of 2 kHz. The EMG signals were stored 200 ms pre-stimulus and 1000 ms post-stimulus. The reflex window was defined from 80 to 150 ms post-stimulus.

Data analysis and Results 5

The data measured in the study described in chapter 4 was analysed to investigate the aim of the project, cf. chapter 3. The processing of the EMG data consisted of normalization, obtaining an envelope of muscle activation, and extraction of muscle synergies. The custom software for the data analysis was written in MATLAB.

5.1 Normalization

EMG signals were normalized in order to make the data comparable between subjects [Halaki and Ginn, 2012]. There are several methods of normalizing data but for this study the normalization for each individual was done by calculating the mean root mean square (RMS) for each muscle across all the 108 trials. The RMS was calculated for each subject for each muscle according to equation (5.1) over the reflex window of N samples:

$$X_{RMS_i} = \sqrt{\frac{1}{N}\sum_{n=1}^{N}|X_i|^2} \tag{5.1}$$

Then the mean RMS was calculated for each sample as shown in equation (5.2)

$$X_{meanRMS,i} = \frac{\sum_{i=1}^{108} X_{RMS_i}}{108} \tag{5.2}$$

Thereafter the EMG data of 108 trials were divided by the corresponding mean RMS for that muscle as seen in equation (5.3).

$$X_{\text{normalized,i}} = \frac{X_i}{X_{meanRMS,i}}, \tag{5.3}$$

where X_i denotes the ith muscle EMG data over all N samples. This normalization resulted in a global feature defined for each EMG channel (muscle) measured.

5.2 Linear Envelope Method

The degree of muscle contraction for generating the desired force is specified by the higher-level control signals originating in the brain and spinal cord [Devarajan and Cheung, 2014].

This is reflected in the envelope of the muscle activation, which is obtained by full-wave rectification and low-pass filtering [Devarajan and Cheung, 2014]. The full-wave rectifier converts the input signal to an output signal with one polarity, either positive or negative. Afterwards the signal is low-pass filtered in order to obtain an envelope of the muscle activation. [Azaripasand et al., 2015]

The raw EMG signal is seen on figure 5.1. In this case the full-wave rectifier returns the absolute values of the EMG signal as seen in figure 5.2. A 4th order Butterworth low-pass filter with a cutoff frequency of 20 Hz [D'Avella et al., 2006] is then applied to the rectified EMG signal in order to obtain the envelope of the muscle activation as seen in Figure 5.3.

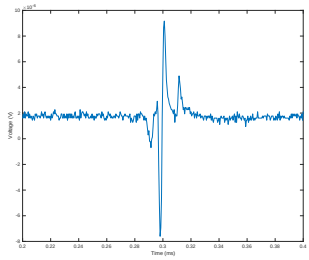

Figure 5.1. Raw

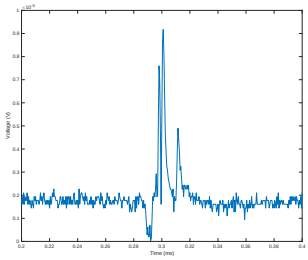

Figure 5.2. Rectified

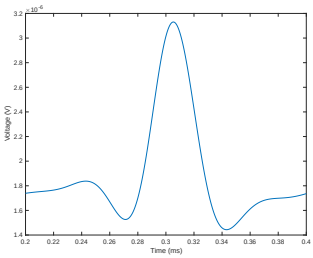

Figure 5.3. Envelope

5.3 Extraction of muscle synergies

To extract the muscle synergies, the NMF method was used. The reason for using NMF was that the synergies were extracted as time-invariant synergy vectors. These were time-invariant and all muscle activity belongs to a single synergy. [Bizzi and Cheung, 2013]

Non-negative Matrix Factorization (NMF) is a mathematical tool of decomposing a non-negative dataset in matrix form into a product of two non-negative matrices. It suits well for decomposing patterns of variability into distinct components and thus can be used to identify muscle synergies from EMG measurements [Burkholder and van Antwerp, 2013].

To extract the muscle synergies, the non-negative matrix factorization (NMF) method was used. The NMF algorithm was implemented with the use of the multiplicative update rule proposed by Lee and Seung [2001] [Wojtara et al., 2014].

NMF reduces the dimensions of a matrix by factorizing the matrix of the recorded EMG data $\mathbf{M}$. $\mathbf{M}$ is factorized into two matrices with only non-negative elements, the synergy matrix $\mathbf{W}$ and the synergy activation coefficients matrix $\mathbf{C}$, and a residual error $\mathbf{D}$ which can contain both negative and positive elements [Berry et al., 2007]. The matrix factorization is given by equation (5.4)

$$\mathbf{M} = \mathbf{WC} + \mathbf{D} \tag{5.4}$$

$\mathbf{M}$ is a $m \times n$ matrix (m = number of measured muscles and n = number of samples), $\mathbf{W}$ is a $m \times k$ (k = number of muscle synergies) and $\mathbf{C}$ is a $k \times n$ matrix [Frère and Hug, 2012]. $\mathbf{D}$ is the residual error between $\mathbf{M}$ and $\mathbf{WC}$, which is minimized by the factors $\mathbf{W}$ and $\mathbf{C}$ [Berry et al., 2007]. $\mathbf{D}$ is given by (5.5)

$$\min_{\mathbf{W},\mathbf{H}} \|\mathbf{M} - \mathbf{WC}\|_F, \quad \text{subject to } \mathbf{W} \geq 0, \mathbf{C} \geq 0 \tag{5.5}$$

where $\|\cdot\|_F$ is the Frobenius norm. An NMF solver (multiplicative update algorithm in MATLAB) was used in order to reconstruct $\mathbf{M}$ from two matrices, $\mathbf{W}$ and $\mathbf{C}$, with the least $\mathbf{D}$. The multiplicative update rule works in iterations of an initial random estimate of $\mathbf{W}$ and $\mathbf{C}$ that converge to a locally optimal matrix factorization [Frère and Hug, 2012]. The number of factorization replicates was 30 for each subject in the algorithm in order to prevent local minima [Shourijeh et al., 2014][Frère and Hug, 2012]. To achieve a consistent extraction of the muscle synergies, the residual convergence criterion and step size was 1e-6 [Burkholder and van Antwerp, 2013; Shourijeh et al., 2014]. From all the replicates, the solution with the minimal error needed to reconstruct the EMG data (i.e. the lowest cost solution) was saved [Frère and Hug, 2012]. The extent of how much the factorized EMG data could reconstruct the input data for the algorithm was determined by the variability accounted for (VAF) [Frère and Hug, 2012; Wojtara et al., 2014]. The mean total VAF was given by (5.6)

$$\text{VAF} = 1 - \frac{\|\mathbf{D}\|_F^2}{\|\mathbf{M}\|_F^2} = 1 - \frac{\sum_{i=1}^{m}\sum_{j=1}^{n}(\mathbf{D}_{i,j})^2}{\sum_{i=1}^{m}\sum_{j=1}^{n}(\mathbf{M}_{i,j})^2} \tag{5.6}$$

The analysis was iterated by varying the number of muscle synergies, k, between 1 and 5. The least value of k at which a VAF above 95 % could be calculated was chosen as the correct number of muscle synergies needed in order to determine $\mathbf{W}$ and $\mathbf{C}$ as representative of the input data $\mathbf{M}$ [Wojtara et al., 2014].

The average muscle activation from the nine trials per intensity in each site was used for the extraction of muscle synergies. Then the average of the synergy matrices and synergy activation coefficients matrices for all 11 subjects was calculated.

5.4 Results

A subject-by-subject analysis of VAF indicated that all 11 subjects had a VAF above 95 % at one or two muscle synergies, therefore two muscle synergies, S1 and S2, accounted for at least 95% of the variability of the EMG data, see figure 5.4.

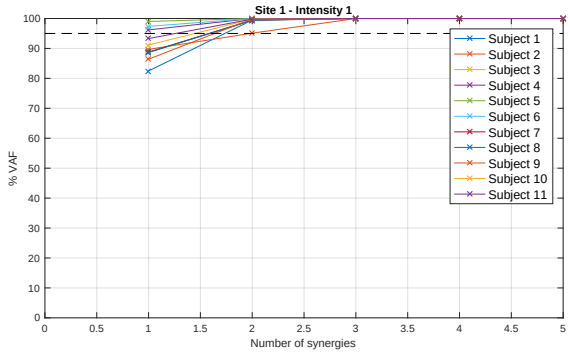

Figure 5.4. Illustrating VAF as a function of the number of muscle synergies on individual trial basis for all 11 subjects.

The $\mathbf{W}$ and $\mathbf{C}$ for each site and intensity were extracted for each subject and averaged over subjects. It was assumed that the contribution of each muscle to a particular synergy over all subjects were normally distributed. The $\mathbf{W}$ for S1 is shown in figure 5.5 with the respective $\mathbf{C}$ in figure 5.6 and for S2 the $\mathbf{W}$ in figure 5.7 and $\mathbf{C}$ in figure 5.8.

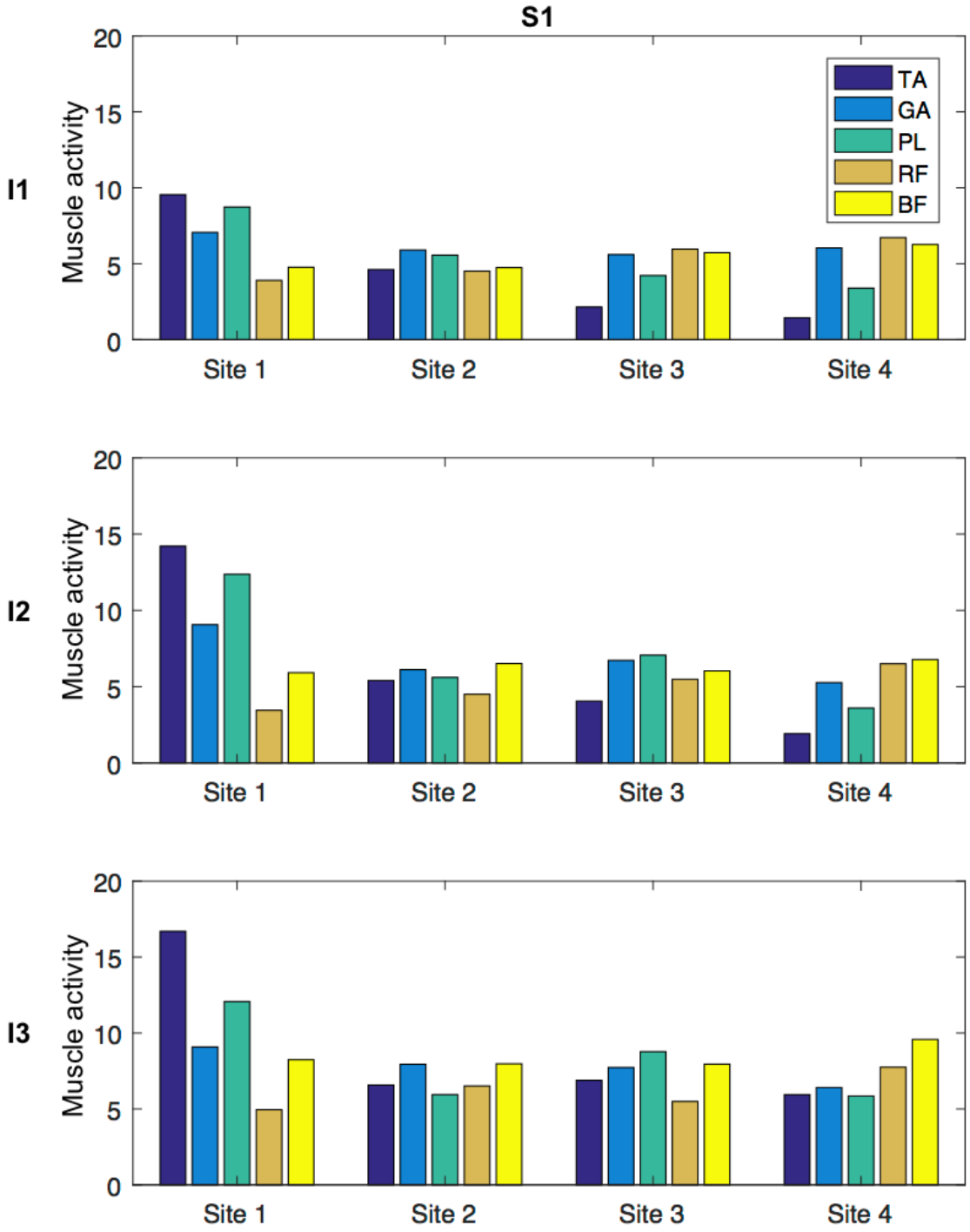

Figure 5.5. The average **W** in S1 over all subjects.

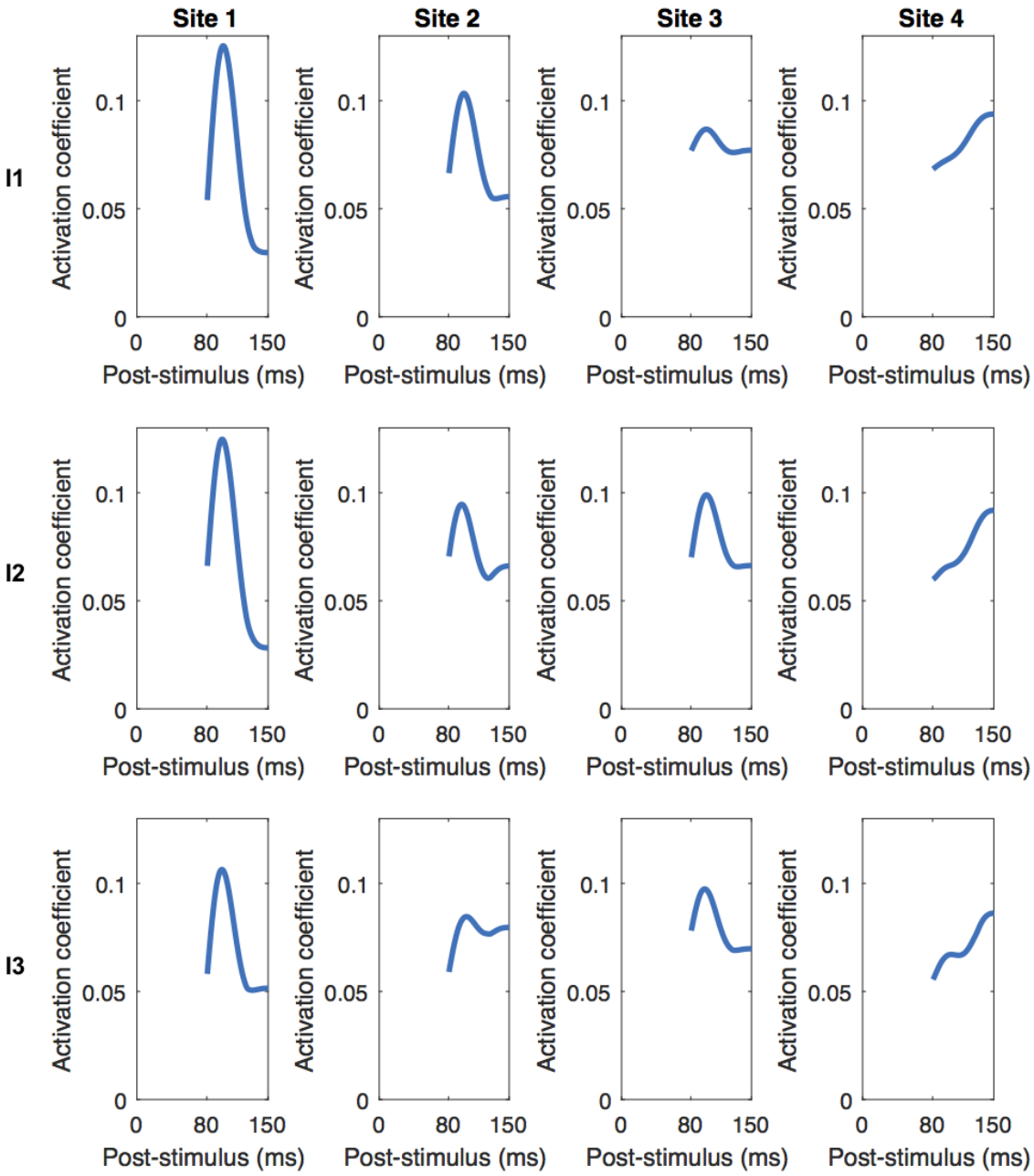

Figure 5.6. The average **C** in S1 over all subjects.

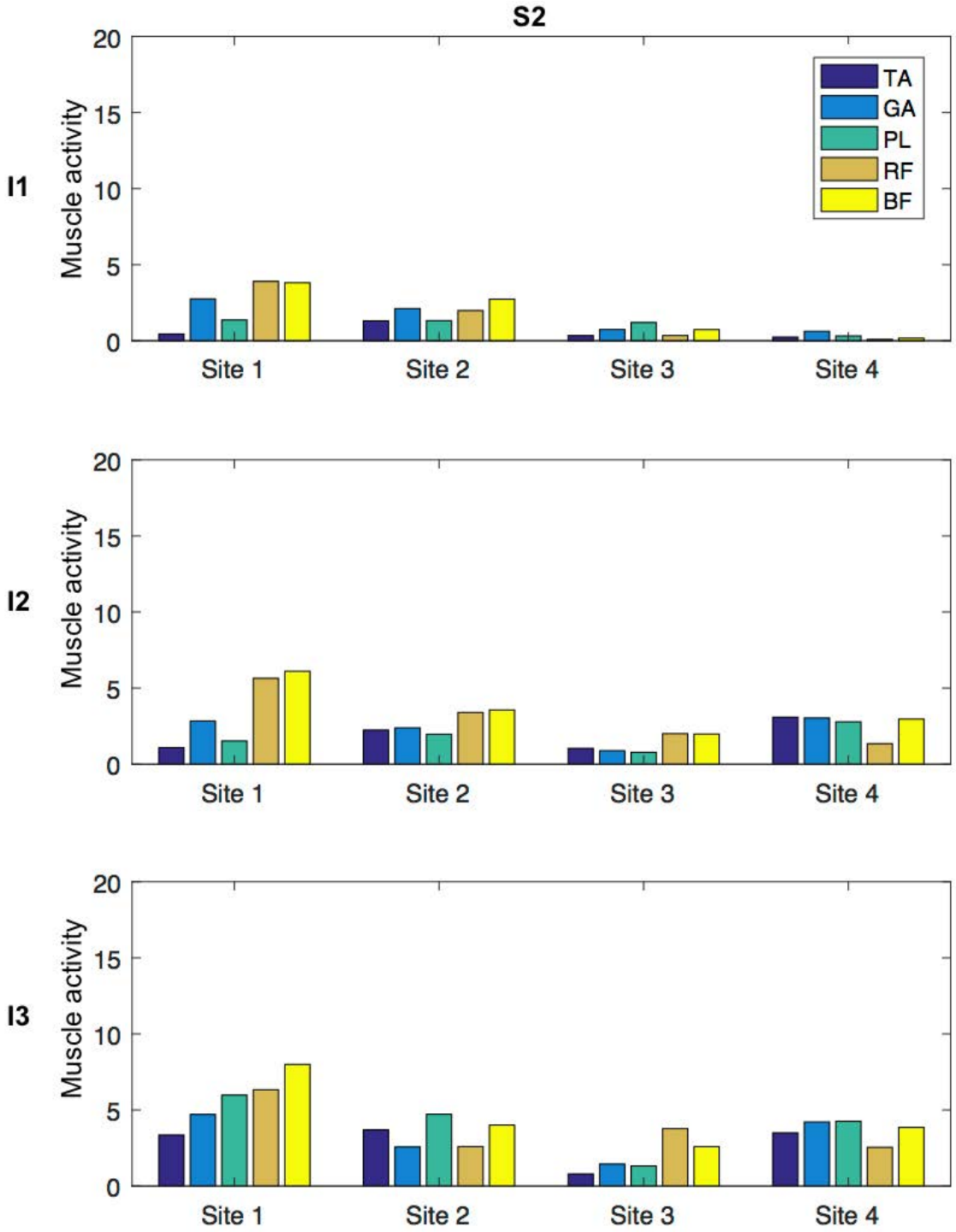

Figure 5.7. The average **W** in S2 over all subjects.

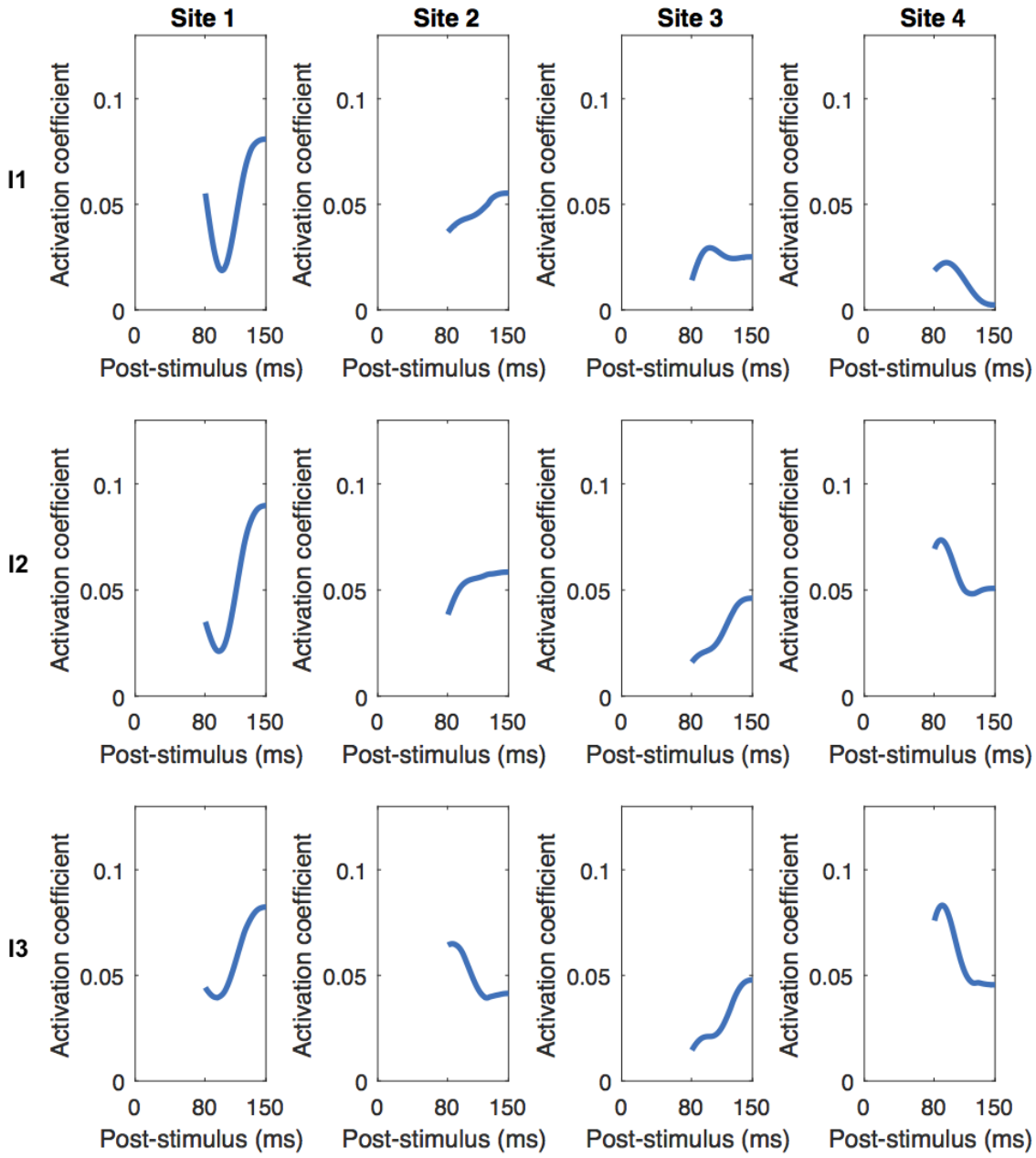

Figure 5.8. The average **C** in S2 over all subjects.

Muscle synergy matrices

The results indicated that in most cases, the mean contributions of the muscles to the synergies were increasing with increasing stimulation intensity and decreasing by changing the sites from 1 to 4. In general, the results showed that on the average over subjects, most of the averaged muscle pattern variability was explained by S1.

The results showed that the muscle activation pattern for all intensities at site 1 had a co-activation of TA and PL in S1. As the sites changed from 1 to 4 the muscle activation pattern changed from a co-activation of TA and PL to a more prominent co-activation of GA, RF and BF at all sites at I1 and I2 for S1. Co-activation is defined by the most active muscles in a synergy. In S1 the muscle activity of TA (at I1 and I2) and PL (at I1) decreased as the stimulation site changed from 1 to 4 but increased in proportion to the intensity. In contrast there was an increase of muscle activity at I1 and I2 as the stimulation site changed from 1 to 4 in GA, RF and BF in S1.

The muscles GA, RF and BF were co-activated only at I1 and I2 for site 1 in S2. Moreover there was an increase of TA and PL at I3. At site 2 the co-activation changed from GA, RF and BF at I1 to TA, GA and BF at I3. The muscle activations at site 3 and site 4 compared to site 1 and site 2 was low at I1. An increase of muscle activity at site 3 and site 4 occurred when the intensity was above the PTh i.e. I2 and I3.

Synergy activations coefficients

The results indicated that site 1 is different from other the sites due to the co-activation of TA and PL shown as a bell shape. In comparison, site 4 showed the co-activation of GA, RF and BF. There is a distinct time activation between S1 and S2 for site 1 compared to the other sites, where no distinct activation coefficient shapes were identified.

Bibliography

Andersen, O. K., Sonnenborg, F. A., and Nielsen, L. A. (1999). Modular organization of human leg withdrawal reflexes elicited by electrical stimulation of the foot sole. *Muscle & Nerve*, 22:1520–1530.

Andersen, O. K., Spaich, E. G., Madeleine, P., and Arendt-Nielsen, L. (2005). Gradual enlargement of human withdrawal reflex receptive fields following repetitive painful stimulation. *Brain Research*, 1042:194–204.

Austin-Community College (2016). Peripheral nervous system- afferent division (somatic). http://www.austincc.edu/apreview/PhysText/PNSafferentpt1.html. [Sidst set d. 01.10.16].

Azaripasand, P., Maleki, A., and Fallah, A. (2015). The extraction of time-varying muscle synergies during hand-reaching movement with a k-means assisted approach. *2015 23rd Iranian Conference on Electrical Engineering*, pages 84–87.

Berry, M. W., Brown, M., Langville, A. N., Pauca, V. P., and Plemmons, R. J. (2007). Algorithms and applications for approximate nonnegative matrix factorization. *Computational Statistics and Data Analysis*, 52(1):155–173.

Birkill, C., van Rensburg, R. J., and Raath, R. (N/A). Electrophysiology and nerve stimulators. *South African Journal of Reginal Anesthesia*, N/A:29–33.

Bizzi, E. and Cheung, V. C. K. (2013). The neural origin of muscle synergies. *Frontiers in Computational Neuroscience*, 7:1–6.

Bjerre, L., Andersen, A., Hagelskjær, M., Ge, N., and Andersen, C. M. O. (2011). Dynamic tuning of human withdrawal reflex receptive fields during cognitive attention and distraction tasks. *European Journal of Pain*, 15:816–821.

Bronzino, J. D. (2000). *The Biomedical Engineering Handbook*. CRC Press, 2nd ed edition.

Burkholder, T. J. and van Antwerp, K. W. (2013). Practical limits on muscle synergy identification by non-negative matrix factorization in systems with mechanical constraints. *Medical & Biological Engineering & Computing*, 51(1):187–196.

Chiodini, L., Adda, G., Scillitani, A., Coletti, F., Morelli, V., Lembo, S. D., Epaminonda, P., Masserini, B., Peccoz, P. B., Orsi, E., Ambrosi, B., and Arosio, M. (2007). Cortisol secretion in patients with type 2 diabetes. *Diabetes Care*, 30:83–88.

D'Avella, A. (2016). *Muscle Synergies*. Encyclopedia of Neuroscience.

D'Avella, A., Portone, A., Fernandez, L., and Lacquaniti, F. (2006). Control of fast-reaching movements by muscle synergy combinations. *The Journal of Neuroscience*, 26(30):7791–7810.

D'Avella, A., Saltiel, P., and Bizzi, E. (2003). Combinations of muscle synergies in the construction of a natural motor behavior. *Nature Neuroscience*, 6:300.

Delsys (2003). *Bagnoli EMG System User Manual*. Delsys Incorporated.

Devarajan, K. and Cheung, V. C. K. (2014). On nonnegative matrix factorization algorithms for signal-dependentnoise with application to electromyography data. *Neural computation*, 26(6):1128–68.

D'Mello, R. and Dickenson, A. H. (2008). Spinal cord mechanisms of pain.

Doucet, M. B., Lam, A., and Griffin, L. (2012). Neuromuscular electrical stimulation for skeletal muscle function. *The Yale journal of biology and medicine*, 85:201–15.

Dowman, R. (1992). Possible startle response contamination of the spinal nociceptive withdrawal reflex. *Pain*, 49:187–197.

Frère, J. and Hug, F. (2012). Between-subject variability ofmuscle synergies during a complex motor skill. *Frontiers in Computational Neuroscience*, 6.

Grimby, L. (1963). Normal plantar response: integration of flexor and extensor reflex components. *Journal of neurology neurosurgery & psychiatry*, 26:39–49.

Halaki, M. and Ginn, K. (2012). Normalization of emg signals: To normalize or not to normalize and what to normalize to? *Intech*, N/A:176–194.

Jensen, M. B., Biurrun, J., and Andersen, O. K. (2015). A new objective method for acquisition and quantification of reflex receptive fields. *Pain*, 156:555–64.

Konrad, P. (2006). *The ABC of EMG*. Noraxon U.S.A. Inc.

Loeser, J. D. and Treede, R.-D. (2008). The kyoto protocol of iasp basic pain terminology. *Elsevier*, 137:473–477.

Luca, C. J. D. (1997). The use of surface electromyography in biomechanics. *Journal of applied biomechanics*, 13:135–163.

Martini, F. H., Nath, J. L., and Bartholemew, E. F. (2014). *Fundamentals of Anatomy and Physiology*. Pearson.

Purves, D., Augustine, G. J., Fitzpatrick, D., Hall, W. C., Anthony-SamuelLamantia, White, L. E., Mooney, R. D., and Platt, M. L. (2012). *Neuroscience*. Sinauer Associates Inc., 5th ed edition.

Rhudy, J. L. and France, C. R. (2007). Defining the nociceptive flexion reflex (nfr) threshold in human participants: A comparison of different scoring criteria. *Pain*, 128:244–253.

Segal, N. A., Boyer, E. R., Teran-Yengle, P., Glass, N., Hillstrom, H. J., and Yack, H. J. (2013). Pregnancy leads to lasting changes in foot structure. *Am J Phys Med Rehabil*, 92:232–240.

SENIAM (2016). Sensor locations.

Shourijeh, M. S., Flaxman, T. E., and Benoit, D. L. (2014). On running non-negative matrix factorization on individual participants for muscle synergies extraction. *Conference: CSCBCE/IEEE EMBS*.

Skljarevski, V. and Ramadan, N. (2002). The nociceptive flexion reflex in humans – review article. *Pain*, 96:3–8.

Torres-Oviedo, G., Macpherson, J. M., and Ting, L. H. (2006). Muscle synergy organization is robust across a variety of postural perturbations. *Journal of neurophysiology*, 96:1530–1546.

Tresch, M. C. and Jarc, A. (2009). The case for and against muscle synergies. *Current Opinion in Neurobiology*, 19:601–607.

Tørring, J., Pedersen, E., and Klemar, B. (1981). Standardisation of the electrical elicitation of the human flexor reflex. *BMJ Publishing Group Ltd*, 44:129.

Winter, D. A. (2009). *Biomechanics and Motor Control of Human Movement*. John Wiley & Sons, Inc., 4th ed edition.

Wojtara, T., Alnajjar, F., Shimoda, S., and Kimura, H. (2014). Muscle synergy stability and human balance maintenance. *Journal of NeuroEngineering and Rehabilitation*, 11.

Muscle Contraction A

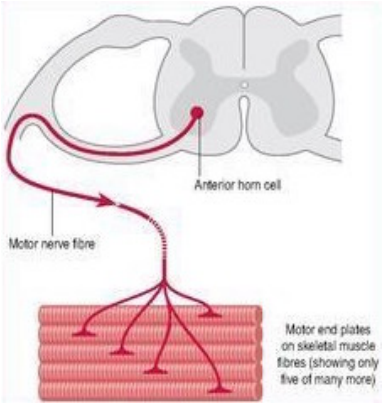

Figure A.1. Overview of a motor unit.

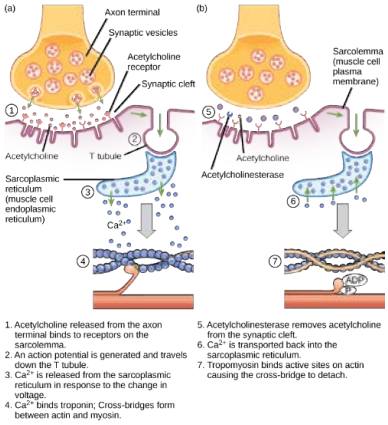

Figure A.2. Illustration of synapse.

A motor unit is described as a somatic neuron (motor neuron) that is connected to muscle fibers by the axons. The axon terminal of a motor neuron contains vesicles with the neurotransmitter acetylcholine (ACh). When an action potential reaches the axon terminal of the motor unit the release of ACh from the vesicles is triggered. The extracellular fluid is filled with sodium ions whereas the inside of the sarcolemma is filled with potassium ions (sodium-potassium pump). When the ACh binds to the ACh-receptor sites located on the sarcolemma the sodium ions enter into the sarcolemma. This causes the gated ion channels to open leading to the generation of excitatory post synaptic potentials (EPSP). Afterwards there is a repolarization phase where the ions move back to their original spaces. This depolarization wave travels along the sarcolemma and reaches the T-tubules, where the calcium ion channels are located. Depolarization of the neuronal membrane potential causes an opening of the calcium ion k channels.